In-depth Analysis of HARQ Performance in Active RIS-assisted RSMA Systems

Yike Zheng, *Student Member, IEEE,* Jie Tang, *Senior Member, IEEE,*
Beixiong Zheng, *Senior Member, IEEE,* Maksim Davydov, and Kai-Kit Wong, *Fellow, IEEE*

***Abstract*—Utilizing reconfigurable intelligent surface (RIS) technology to construct intelligent radio environments is a prerequisite for developing the sixth-generation (6G) communication networks characterized by ultra-high speed, minimal latency, and extensive connectivity. Therefore, to further enhance the coverage and robustness of wireless communication systems, we investigate an active RIS-assisted rate-splitting multiple access (RSMA) system. Specifically, we examine the effect of relevant parameters on system performance by deriving the analytical expressions of the outage probability (OP) for users employing hybrid automatic repeat request (HARQ) transmission protocol. The numerical results indicate that: 1) Implementing the HARQ transmission protocol can boost signal quality and improve system reliability. 2) The increase in the number of reconfigurable elements also significantly enhances the stability performance of the considered system.**

***Index Terms*—Active reconfigurable intelligent surface (RIS), rate-splitting multiple access (RSMA), hybrid automatic repeat request (HARQ), outage probability (OP).**

I. Introduction

THE continuous pursuit of increased data rates, ultra-reliable low-latency communication (URLLC), and extensive device connectivity is driving the development of the sixth-generation (6G) wireless network technology [1]. Yet, realizing these goals is fundamentally contingent upon advancing technologies capable of overcoming the inherent challenges in wireless communication systems [2]. Reconfigurable intelligent surface (RIS) have emerged as disruptive solutions, offering an intelligent and adaptive wireless environments to achieve the goals of 6G networks. Specifically, RIS adjusts the phase shifts and/or amplitudes of incoming radio frequency (RF) signals via reflection, thus enhancing reception at targeted destinations as well as minimizing interference for unintended users [3]. RIS markedly improves signal coverage and quality over conventional wireless communication technologies, boosting spectral efficiency and fostering innovative, energy-efficient communication solutions [4]–[6].

For RIS-assisted wireless communication systems, the signals reflected by RIS traverse two transmission paths: the source-RIS path and the RIS-destination path. Consequently, the signal arriving at the destination undergoes dual-path loss attenuation, markedly limiting the coverage range of the system. To mitigate this challenge, the notion of active RIS has been proposed as a solution in [7]. Active RIS with built-in amplifiers strengthens signals to effectively mitigate dual-path loss attenuation, enhancing communication quality over long distances or in areas with substantial signal degradation. This boosts wireless spectrum efficiency and elevates overall system performance [8]. Therefore, active RIS has garnered significant research interest within the academic community in recent years [9], [10]. In [9], a proposal was made for an active RIS-assisted multi-user system, aiming to optimize collectively the transmit beamforming reflection precoding to maximize the overall sum rate of the considered system. To further enhance transmission rates and effectively ensure user fairness, Yang *et al.* in [10] delved into the transmission rate optimization problem for RIS-assisted downlink non-orthogonal multiple access (NOMA) system, employing block coordinate descent and semidefinite relaxation techniques to achieve rate maximization for all users.

With the swift advancement of wireless communication technologies, the rapid spread of various applications, and the sharp increase in data traffic, the demand for efficient and reliable connectivity solutions has become increasingly critical. In this context, rate-splitting multiple access (RSMA) emerges as a beneficial technology, offering unique benefits in managing communication resources and meeting the diverse demands of wireless networks [11]. Specifically, RSMA, based on linear precoding rate splitting, exhibits capabilities in mitigating partial decoding interference and managing partial interference by treating it as noise [12]. Despite the certain advantages offered by introducing RSMA, establishing reliable communication links over rapidly changing wireless channels remains a challenge. To tackle this issue, researchers have conducted extensive research on the collaboration between RSMA and RIS systems to optimize signal transmission and reception. This enhances the system's robustness against imperfect CSI while effectively reducing the computational complexity of the system [13], [14]. Using RIS technology, single-layer RSMA can match the performance of multi-layer RSMA,

This work was supported in part by the National Natural Science Foundation of China under Grant 62222105, Grant 62201214 and Grant 62331022; in part by the Natural Science Foundation of Guangdong Province under Grant 2023A1515011753; and in part by the Fundamental Research Funds for the Central Universities under Grant 2023ZYGXZR106. *(Corresponding author: Jie Tang.)*

Y. Zheng and J. Tang are with the School of Electronic and Information Engineering, South China University of Technology, Guangzhou 510640, China (e-mail:eeykzheng@mail.scut.edu.cn; eejtang@scut.edu.cn).

B. Zheng is with the School of Microelectronics, South China University of Technology, Guangzhou 511442, China (e-mail: bxzheng@scut.edu.cn).

M. Davydov is with the School of Electrical Engineering Theory, Belarusian State University of Informatics and Radioelectronics, 220012 Minsk, Belarus (e-mail:davydovmax@gmail.com).

K. K. Wong is affiliated with the Department of Electronic and Electrical Engineering, University College London, Torrington Place, WC1E 7JE, United Kingdom and he is also affiliated with Yonsei Frontier Lab, Yonsei University, Seoul, Korea (e-mail: k.wong@ee.ucl.ac.uk).

with simpler signal processing that lowers the communication system's computational complexity and concurrently boosts performance [13]. To further maximize the energy efficiency of RIS-assisted RSMA communication system, Narottama *et al.* in [14] proposed a quantum machine learning algorithm.

The hybrid automatic repeat request (HARQ) technology, by strategically retransmitting information a limited number of times, aims to mitigate data loss due to channel fading, thereby significantly enhancing the reliability and efficiency of data transmission [15]. Considering this, to strengthen the overall stability of wireless communication systems, especially in complex and variable Internet-of-Things (IoT) scenarios, combining HARQ with RIS technology is anticipated to fortify the overall stability of wireless communication systems and meet various communication goals, such as improving transmission quality, enhancing system reliability, and reducing latency [16]. This integrated approach has attracted the attention of researchers [17], [18]. To improve the efficiency of the considered system, the authors in [17] have employed HARQ scheme and conducted the effective capacity performance analysis on RIS-supported D2D links facilitated by HARQ. In [18], Abidrabbu *et al.* proposed an efficient HARQ transmission protocol tailored for RSMA networks, analyzing the efficacy of three newly introduced retransmission strategies.

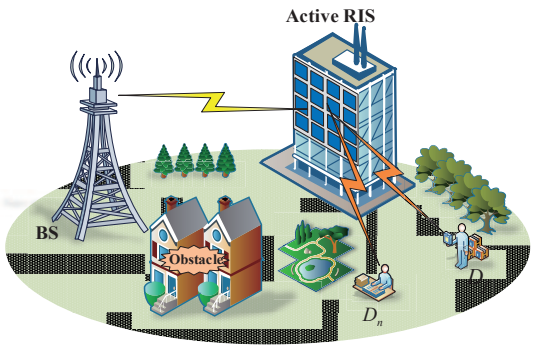

Fig. 1. System model of active RIS-assisted RSMA.

Although discussions on related technologies have been conducted, the specific impact and effectiveness of HARQ performance within active RIS-assisted RSMA systems has yet to be reached a consensus. Ensuring the reliability of signal transmission in complex and obstacle-laden wireless communication environments, while avoiding significant increases in computational complexity, remains an urgent research issue to be addressed. To effectively tackle this challenge, this paper uses the OP as a core metric to assess the HARQ performance and analyzes the reliability performance of users in an active RIS-assisted RSMA network. Specifically, with the support of RIS, RSMA architecture effectively mitigates propagation barriers and communication congestion while reducing computational complexity, enhancing system robustness. Compared to passive RIS, active RIS can amplify signals and suppress noise, enhancing signal transmission, mitigating multipath fading, and significantly improving the system's capacity, reliability, and coverage range [19]. Additionally, by integrating the HARQ retransmission protocol, the system effectively suppresses performance fluctuations caused by channel uncertainty without inducing additional transmission delays, enhancing system stability. Through theoretical analysis and simulation validation, this paper demonstrates the integration of the HARQ protocol effectively enhances the stability of signal transmission within the network.

II. System Model

Fig. 1 depicts an active RIS-assisted RSMA system, comprising of a BS, an active RIS, a far user (labeled as D_f), and a near user (labeled as D_n). Specifically, the RIS is furnished with N reflective elements, and each user is outfitted with a single antenna. In complex urban communication environments characterized by severe channel blockages, the deploying active RIS is crucial for maintaining stable communication links between the BS and users. Furthermore, all channels are modeled following the Rician fading distribution. To enhance the reliability of information transmission within the system, the HARQ protocol is implemented, whereby data packets not successfully decoded are scheduled for retransmission, with a maximum retransmissions limit of L for the required signals. Besides, the channel coefficients for the BS-RIS link, RIS-D_f link, and RIS-D_n link during the l-th ($1 \leq l \leq L$) round retransmission are denoted by $\left(\mathbf{h}_{sr}^{l}\right)^{H} = \left[h_{sr_1}^{l}, h_{sr_2}^{l}, \ldots, h_{sr_N}^{l}\right] \in \mathbb{C}^{1\times N}$, $\mathbf{h}_{rf}^{l} = \left[h_{rf_1}^{l}, h_{rf_2}^{l}, \ldots, h_{rf_N}^{l}\right]^{H} \in \mathbb{C}^{N\times 1}$, and $\mathbf{h}_{rn}^{l} = \left[h_{rn_1}^{l}, h_{rn_2}^{l}, \ldots, h_{rn_N}^{l}\right]^{H} \in \mathbb{C}^{N\times 1}$, with their respective fading parameters being K_{sr}, K_{rf}, and K_{rn}. Following the Rician fading criterion, h_j^l, $j \in (sr, rj, rn)$ can be modeled as:

$$h_j^l = \sqrt{d_j^{-\varepsilon_j}}\left(\sqrt{\frac{K_j}{K_j+1}}\bar{h}_j^l + \sqrt{\frac{1}{K_j+1}}\tilde{h}_j^l\right), \quad (1)$$

where $\bar{h}_j^l$ represents the normalized deterministic component of the line-of-sight (LoS), i.e., $\left|\bar{h}_j^l\right| = 1$; $\tilde{h}_j^l$ represents the non-line-of-sight (NLoS) components characterized by a complex Gaussian distribution, while $\tilde{h}_j^l \sim \mathcal{CN}(0,1)$; d_j corresponds to the transmission distance of the respective link. Another key parameter in our analysis is $-\epsilon_j$, which directly corresponds to the path loss characteristics of the respective link.

Considering the RSMA technology, the signal emitted by the BS can be represented as:

$$x_s = \sqrt{\alpha_a P_s}x_a + \sum_{k=1}^{2}\sqrt{\alpha_{p,k}P_s}x_{p,k}, \quad (2)$$

where P_s denotes the transmission power of the BS; x_a represents the common message with α_a denoting its power allocation parameter; $x_{p,1}$ and $x_{p,2}$ respectively signify the private messages for D_f and D_n, with $\alpha_{p,1}$ and $\alpha_{p,2}$ corresponding to their respective power allocation parameters, and $\alpha_a + \alpha_{p,1} + \alpha_{p,2} = 1$. To ensure the security of the private message $x_{p,k}$ ($k \in \{1,2\}$), it is assumed that $\alpha_a > 0.5$. Moreover, given that D_n has favorable channel conditions, it is assumed that $\alpha_{p,1} > \alpha_{p,2}$.

Utilizing the HARQ scheme, l is set to 1 for the initial transmission. If the receiver fails to decode the packet successfully, it sends a negative acknowledgement (NACK) signal, l is incremented, and a retransmission is requested. This process continues until the receiver successfully decodes the packet

(sends an acknowledgement (ACK) signal) or l reaches L. Consequently, the signal received by the users D_i ($i \in \{f, n\}$) can be expressed as follows:

$$y_{i,l} = \left(\mathbf{h}_{sr}^{l}\right)^{H} \Lambda \mathbf{h}_{ri}^{l} x_s + \mathbf{h}_{ri}^{l} \Lambda n_r + n_i, \tag{3}$$

where $\Lambda = diag\left(\beta_1 e^{j\theta_1}, \ldots, \beta_n e^{j\theta_n}, \ldots, \beta_N e^{j\theta_N}\right)$ denotes the phase shift matrix of the active RIS, where $\beta_n > 0$ and $\theta_n \in [0, 2\pi)$ stand for the reflection coefficient and phase shift of the n-th reflecting element, respectively. For passive RIS, $0 < \beta_n < 1$ must be satisfied. However, for active RIS, due to its amplifiers, $\beta_n > 1$ is achievable. Due to the thermal noise generated by the active RIS, $n_r \sim \mathcal{CN}\left(0, \sigma_r^2\right)$ cannot be neglected. Besides, $n_i \sim \mathcal{CN}\left(0, \sigma_i^2\right)$ stands for the additive complex Gaussian white noise at D_i.

A. Received signal-to-interference-plus-noise

Based on the aforementioned analysis and under the assumption of perfect channel state information within the system, it is hypothesized that, in the context of RSMA network transmission characteristics, D_i ($i \in \{f, n\}$) initially decodes the common message. Consequently, the signal-to-interference-plus-noise ratio (SINR) for decoding the common message x_c at D_i is expressed as:

$$\gamma_{D_i}^{c} = \frac{\alpha_a P_s \left[\left(\mathbf{h}_{sr}^{l}\right)^{H} \mathbf{Q} \mathbf{h}_{ri}^{l}\right]^2}{\sum_{k=1}^{2} \alpha_{p,k} P_s \left[\left(\mathbf{h}_{sr}^{l}\right)^{H} \mathbf{Q} \mathbf{h}_{ri}^{l}\right]^2 + \left(\mathbf{h}_{ri}^{l} \mathbf{Q}\right)^2 \sigma_r^2 + \sigma_i^2}. \tag{4}$$

Adhering to the RSMA transmission protocol, once the common message is successfully decoded, D_f and D_n proceed to decode their respective private messages. Thus, the SINR for decoding $x_{p,1}$ at D_f and $x_{p,2}$ at D_n can be depicted as:

$$\gamma_{D_f}^{p} = \frac{\alpha_{p,1} P_s \left[\left(\mathbf{h}_{sr}^{l}\right)^{H} \mathbf{Q} \mathbf{h}_{rf}^{l}\right]^2}{\alpha_{p,2} P_s \left[\left(\mathbf{h}_{sr}^{l}\right)^{H} \mathbf{Q} \mathbf{h}_{rf}^{l}\right]^2 + \left(\mathbf{h}_{rf}^{l} \mathbf{Q}\right)^2 \sigma_r^2 + \sigma_f^2}, \tag{5}$$

and

$$\gamma_{D_n}^{p} = \frac{\alpha_{p,2} P_s \left[\left(\mathbf{h}_{sr}^{l}\right)^{H} \mathbf{Q} \mathbf{h}_{rn}^{l}\right]^2}{\alpha_{p,1} P_s \left[\left(\mathbf{h}_{sr}^{l}\right)^{H} \mathbf{Q} \mathbf{h}_{rn}^{l}\right]^2 + \left(\mathbf{h}_{rn}^{l} \mathbf{Q}\right)^2 \sigma_r^2 + \sigma_n^2}. \tag{6}$$

B. Channel Statistics

As previously mentioned, the pertinent channel coefficients adhere to the Rician fading distribution. Consequently, the probability density function (PDF) for h_j^l, $j \in (sr, rj, rn)$ can be represented as:

$$f_{\left|h_j^l\right|}(x) = \frac{2x\varpi_1}{e^{K_j}} e^{-x^2 \varpi_1} I_0\left(2x\sqrt{K_j \varpi_1}\right), \tag{7}$$

where $\eta_j = d_j^{-\varepsilon_j}$, $\varpi_1 = \frac{K_j+1}{\eta_j}$, and $I_0(\cdot)$ refers to the zeroth-order modified Bessel function of the first kind.

In the implementation of coherent phase shifting, the phase shift of each reflecting element is adjusted to match the phase of the associated fading channel, significantly boosting network performance. Hence, similar to [20], the coherent phase shifting strategy is employed for managing the cascaded channels.

Theorem 1: Assume that the cascaded channel propagated through RIS [21] is represented as $A_{i,k}^{l} = h_{sr}^{l} h_{ri_k}^{l}$, Where $i \in (f, n)$ and $l \in \{1, 2, \ldots, L\}$ represents the l-th round retransmission. Then the PDF of $A_{i,k}^{l}$ can be represented in (8), which is displayed at the top of subsequent page. Noted that in (8), $K_v(\cdot)$ represents the second-kind modified Bessel function with order v.

However, analysis indicates that obtaining the expression of PDF for $Z = \sum_{k=1}^{N} A_{i,k}^{l}$ presents certain challenges. Consequently, an approximation of its PDF is derived by employing Laguerre polynomials [22]. Then the PDF of Z can be represented as

$$f_Z(z) \approx \frac{z^{\varphi_i - 1}}{\psi_i^{\varphi_i} \Gamma(\varphi_i)} \mathrm{e}^{-\frac{z}{\psi_i}}, \tag{9}$$

where $\varphi_i = \frac{\left(\mu_{si}^{l}\right)^2 N}{\nu_{si}^{l}}$, and $\psi_i = \frac{\nu_{si}^{l}}{\mu_{si}^{l}}$. $\mu_{si}^{l} = \mathbb{E}\left(A_{i,k}^{l}\right) = \frac{\pi}{4\sqrt{(K_{sr}+1)(K_{ri}+1)}} L_{\frac{1}{2}}(-K_{sr}) L_{\frac{1}{2}}(-K_{ri})$ and $\nu_{si}^{l} = \mathbb{D}\left(A_{i,k}^{l}\right) = 1 - \frac{\pi^2}{16(1+K_{sr})(1+K_{ri})}\left[L_{\frac{1}{2}}(-K_{sr}) L_{\frac{1}{2}}(-K_{ri})\right]^2$ denote the expected value and variance of A_i^l, respectively; $L_{\frac{1}{2}}(K) = e^{\frac{K}{2}}\left[(1-K) I_0\left(-\frac{K}{2}\right) - K I_1\left(-\frac{K}{2}\right)\right]$ is the Laguerre polynomial. $I_1(\cdot)$ generally represents the modified Bessel function of the first kind, specifically of order 1.

III. Performance Analysis

In this section, through the derivation of the analytical expression for the OPs of the system under consideration, we analyze the HARQ performance in active RIS-assisted RSMA network. More specifically, the OP is characterized as the probability of the event where the cumulative mutual information (I) received at the destination falls below the transmission rate (R). Hence, the OP can be expressed as:

$$P_{out} = \Pr(I < R), \tag{10}$$

Under the operation of HARQ, BS continuously transmits new signals from independent random codebook to $D_i, i \in (f, n)$ until an ACK is received or the maximum transmission rounds, L, are reached. Consequently, the analytic expression for OP of D_i, can be further transformed into

$$P_{out}^{i} = \left[1 - \Pr\left(\gamma_{D_i}^{c} > \theta_i^{c}, \gamma_{D_i}^{p} > \theta_i^{p}\right)\right]^L = \left(1 - P_{i,l}^{o}\right)^L, \tag{11}$$

where $\theta_i^c = 2^{R_c^i} - 1$, $\theta_i^p = 2^{R_p^i} - 1$, R_c^i stands for the threshold transmission rate of D_i for the message x_c, and R_p^i represents the threshold transmission rate of D_i for the private message $x_{p,k} (k \in \{1, 2\})$. $P_{i,l}^{o}$ represents the probability that the signal is successfully decoded in the l-th transmission round.

Theorem 2: In case of the Rician fading channels, the analytical expression for the P_f^l of D_f, after a series of calculations, can be summarized in (12), which is displayed at the top of next page. Noted that in (12), $\mu_f^l = \mathbb{E}\left(h_{rf_k}^{l}\right) = \frac{\sqrt{\pi}}{2\sqrt{(K_{rf}+1)}} L_{\frac{1}{2}}(-K_{rf})$ and $\nu_f^l = \mathbb{D}\left(h_{rf_k}^{l}\right) = 1 - \frac{\pi}{4(1+K_{rf})}\left[L_{\frac{1}{2}}(-K_{rf})\right]^2$ signify the mean and variance of $h_{rf_k}^{l}$, respectively. $\Delta_f = \max\left(\frac{\theta_f^c}{\alpha_a \gamma_s B_{sf} - (\alpha_{p,1}+\alpha_{p,2})\gamma_s B_{sf} \theta_f^c}, \frac{\theta_1^p}{\alpha_{p,1}\gamma_s B_{sf} - \alpha_{p,2}\gamma_s B_{sf}\theta_f^c}\right)$, $\gamma_s = \frac{P_s}{\sigma_f^2}$, $\gamma_r = \frac{P_s}{\sigma_r^2}$, $\varphi_f^l = \frac{N\left(\mu_f^l\right)^2}{\nu_f^l}$, $\psi_f^l = \frac{\nu_f^l}{\mu_f^l}$,

$$f_{|A_{i,k}^l|}(x)=\sum_{t=0}^{\infty}\sum_{m=0}^{\infty}\frac{4x^{t+m+1}(K_{sr}+1)^{t+1}(K_{ri}+1)^{m+1}K_{sr}^{t}K_{ri}^{m}}{(t!)^2(m!)^2e^{K_{sr}+K_{ri}}(\eta_{sr}\eta_{ri})^{\frac{t+m+2}{2}}}K_{t-m}\left(2x\sqrt{\frac{(K_{sr}+1)(K_{ri}+1)}{\eta_{sr}\eta_{ri}}}\right). \tag{8}$$

$$P_f^l=\begin{cases}\sum\limits_{j=0}^{\infty}\frac{\varphi_f^j e^{-\frac{\varphi_f}{2}}}{j!2^j}\left(1-\sum\limits_{m=0}^{\infty}\sum\limits_{t=0}^{\infty}\frac{(-1)^t\pi W\sqrt{1-\vartheta_f^2}\,g_f^{\varphi_f^l-1}\Delta_f^{C_1}(g_f\gamma_r B_{rf}+1)^{C_1}e^{-\frac{g_f}{\psi_f^l}}}{2M\left(2N\nu_{sf}^l\right)^{C_1}\Gamma\left(j+\frac{1}{2}\right)t!(C_1)\Gamma\left(\varphi_f^l\right)\left(\psi_f^l\right)^{\varphi_f^l}}\right), \theta_f^c<\frac{\alpha_{p,1}}{\alpha_{p,1}+\alpha_{p,2}}, \theta_1^c<\frac{\alpha_{p,1}}{\alpha_{p,2}}\\ 1, otherwise\end{cases}, \tag{12}$$

$\vartheta_f = \frac{\cos[(2m-1)\pi]}{2M}$, $g_f = \frac{W\vartheta_f}{2}$, $C_1 = j+t+\frac{1}{2}$, $B_{sf} = \eta_{sr}\eta_{rf}\beta^2$, and $B_{rf} = \eta_{rf}\beta^2$. Besides, W and M both represent numerically large real numbers.

Proof: Substituting (4), (5), and (9) into (11) yields the result of (12). ∎

Theorem 3: In case of the Rician fading channels, after a series of computations, the analytical expression for the P_n^l of D_n can be succinctly expressed as (13), which is displayed at the top of subsequent page. Noted that in (13), $\varphi_n^l = \frac{N\left(\mu_n^l\right)^2}{\nu_n^l}$, $\psi_n^l = \frac{\nu_n^l}{\mu_n^l}$, $\Delta_n = \max(\frac{\theta_n^c}{\alpha_a\gamma_s B_{sn}-(\alpha_{p,1}+\alpha_{p,2})\gamma_s B_{sn}\theta_n^c}, \frac{\theta_2^p}{\alpha_{p,2}\gamma_s B_{sn}-\alpha_{p,1}\gamma_s B_{sn}\theta_n^c})$, $\vartheta_n = \frac{\cos[(2m-1)\pi]}{2G}$, $g_n = \frac{R\vartheta_n}{2}$, $C_2 = z+u+\frac{1}{2}$, $B_{sn} = \eta_{sr}\eta_{rn}\beta^2$, $B_{rn} = \eta_{rn}\beta^2$, $\nu_n^l = \mathbb{D}\left(h_{rn_k}^l\right) = 1-\frac{\pi}{4(1+K_{rn})}\left[L_{\frac{1}{2}}\left(-K_{rn}\right)\right]^2$ and $\mu_n^l = \mathbb{E}\left(h_{rn_k}^l\right) = \frac{\sqrt{\pi}}{2\sqrt{(K_{rn}+1)}}L_{\frac{1}{2}}\left(-K_{rn}\right)$ signify the mean and variance of $h_{rn_k}^l$, respectively. Besides, R and G both represent numerically large real numbers.

Remark 1: Theorems 2 and 3 indicate that as P_s increases, the OPs for D_f and D_n decrease, thereby improving the reliability performance of the considered system. Additionally, the reliability performance of both users is positively influenced by the number of retransmission attempts. Specifically, as the number of retransmission (L) increases, the probability of successful signal decoding also rises, which in turn enhances the reliability performance of the considered system. Lastly, adding more the number of reflecting elements in the active RIS further contributes to improving the overall performance of the system.

TABLE I
TABLE OF THE RELEVANT PARAMETERS FOR THE CONSIDERED SYSTEM IN NUMERICAL ANALYSIS.

Relevant parameters	Numerical results
Power allocation parameter	$\alpha_c = 0.6$, $\alpha_{p,1} = 0.3$, $\alpha_{p,2} = 0.1$
Element reflecting parameter	$\beta^2 = 9$
Transmission distance	$d_{sr} = 18$m, $d_{rf} = 12$m, $d_{rn} = 8$m
Path loss exponent	$\varepsilon_{sr} = \varepsilon_{rf} = 2.3$, $\varepsilon_{rn} = 2.5$
Number of reflecting elements	$N = 16$
Rician parameter	$K_{sr} = K_{rf} = K_{rn} = K = -1$dB
Retransmission times	$L = 3$
Threshold for transmission rate	$R_c^{l,f} = R_c^{l,n} = R_p^{l,f} = R_p^{l,n} = 0.001$

IV. Numerical Results

In this section, Monte Carlo simulations consisting of 10^5 iterations are utilized to confirm the accuracy of the analyses conducted in Section III. The parameters are configured as described in Table I, unless indicated differently.

Fig. 2 shows the trend of OP for D_f and D_n with respect to P_s. Specifically, we can observe that the OP for D_f and D_n decreases as P_s increases. This trend indicates that the reliability performance of both users increases with the increase of P_s. In addition, we also found that D_f has better reliability performance than D_n. This is because D_f is allocated more transmission power, resulting in more reliable transmission performance. Through comparative analysis of system reliability performance under different retransmission times L, we observed that as L increases, the system provides more redundant information, enabling the receiver to correct erroneous data more accurately and effectively. Additionally, the combination of the dynamic channel adjustment technology of active RIS and the resource allocation mechanism of RSMA, reliability performance is enhanced for both types of users. This result indicates that the introduction of the HARQ protocol significantly improves the overall reliability of the network.

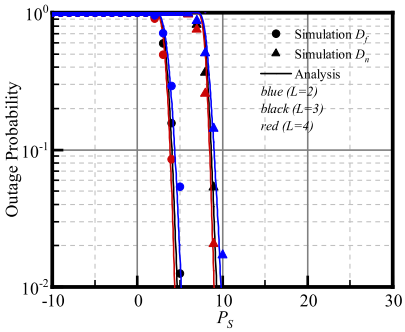

Fig. 2. The OP of D_f and D_n versus P_s under different retransmission times.

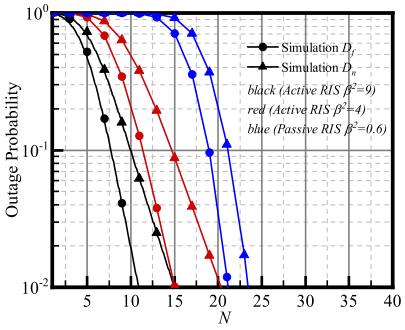

Fig. 3. The OP for D_f and D_n versus the number of reflecting elements under different β.

Fig. 3 demonstrates the OP versus the number of reflecting elements N with $P_s = 10$dBm , $d_{rn} = 10$m and $\beta^2 = 4$. Specifically, as the number of reflecting elements increases, the channel gain is significantly enhanced, and the signal quality

$$P_n^l = \begin{cases} \sum_{z=0}^{\infty} \left(\frac{\left(\varphi_n^l\right)^z e^{-\frac{\varphi_n}{2}}}{z! 2^c} - \sum_{m=0}^{\infty} \sum_{u=0}^{\infty} \frac{(-1)^u \pi R \sqrt{1-\vartheta_n^2} \left(\varphi_n^l\right)^p [\Delta_n (g_n \gamma_r B_{rn}+1)]^{C_2} e^{-\frac{g_n}{\psi_n^l} - \frac{\varphi_n}{2}}}{2^{z+1} z! u! G C_2 (2N\nu_{sn}^l)^{C_2} g_n^{1-\varphi_n^l} \Gamma\left(z+\frac{1}{2}\right) \Gamma(\varphi_n^l)(\psi_n^l)^{\varphi_n^l}} \right), \theta_n^c < \frac{\alpha_{p,2}}{\alpha_{p,1}+\alpha_{p,2}}, \theta_2^q < \frac{\alpha_{p,2}}{\alpha_{p,1}} \\ 1, otherwise \end{cases}, \quad (13)$$

is improved, thereby reducing the OPs of signal transmission. Additionally, with the increase in reflecting parameters, the RSMA system can utilize channel resources more efficiently, significantly enhancing system reliability. Similarly, the active RIS-assisted RSMA system exhibits better transmission characteristics compared to the passive RIS-assisted RSMA system. This is because active RIS units amplify signal, effectively boosting signal strength and increasing channel capacity, thereby markedly improving overall system reliability. These findings align with the conclusions shown in Fig. 2, since under the same conditions, D_f demonstrates higher transmission power, thus offering better reliability performance than D_n.

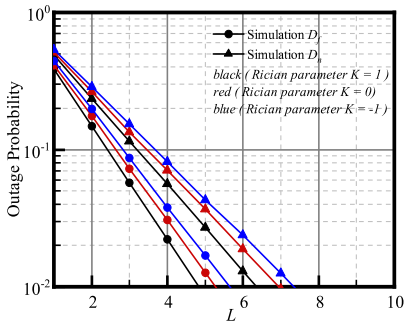

Fig. 4. The trend of OP for D_f and D_n versus L.

Fig. 4 plots the OP for D_f and D_n versus L with $P_s = 9$dBm and $\beta^2 = 4$. Apparently, with the increase of the number of retransmission times L, the decrease in OP leads to a notable enhancement in system reliability. Similarly, from another perspective, as K increases, representing the predominance of the LoS component in the time-domain fading channels, this leads to improved channel conditions and thus enhanced reliability performance.

V. Conclusion

In this letter, we investigated an active RIS-assisted RSMA network to ensure effective signal transmission in obstructed wireless communication environments. We explored the reliability performance of the considered network under the HARQ scheme by deriving the analytic expressions of the OP for users. The effects of transmitting power, HARQ retransmission times, the number of reflective factor and reconfigurable elements in RIS on system performance were studied. The numerical results indicate that the stability performance of the considered system can be significantly enhanced by introducing HARQ protocol.

References

[1] L. Zhang, Y.-C. Liang, and D. Niyato, "6G visions: Mobile ultra-broadband, super internet-of-things, and artificial intelligence," *China Communications*, vol. 16, no. 8, pp. 1–14, 2019.

[2] W. Saad, M. Bennis, and M. Chen, "A vision of 6G wireless systems: Applications, trends, technologies, and open research problems," *IEEE Netw.*, vol. 34, no. 3, pp. 134–142, Oct. 2020.

[3] R. Ma, J. Tang, X. Zhang, K.-K. Wong, and J. A. Chambers, "Energy-efficiency optimization for mutual-coupling-aware wireless communication system based on RIS-enhanced SWIPT," *IEEE Internet of Things Journal*, vol. 10, no. 22, pp. 19 399–19 414, Nov. 2023.

[4] M. Di Renzo, A. Zappone, M. Debbah, M.-S. Alouini, C. Yuen, J. de Rosny, and S. Tretyakov, "Smart radio environments empowered by reconfigurable intelligent surfaces: How it works, state of research, and the road ahead," *IEEE J. Sel. Areas Commun.*, vol. 38, no. 11, pp. 2450–2525, Jul. 2020.

[5] Y. Liu, X. Liu, X. Mu, T. Hou, J. Xu, M. Di Renzo, and N. Al-Dhahir, "Reconfigurable intelligent surfaces: Principles and opportunities," *IEEE Commun. Surv. Tutorials*, vol. 23, no. 3, pp. 1546–1577, May 2021.

[6] Z. Chen, G. Chen, J. Tang, S. Zhang, D. K. So, O. A. Dobre, K.-K. Wong, and J. Chambers, "Reconfigurable-intelligent-surface-assisted B5G/6G wireless communications: Challenges, solution, and future opportunities," *IEEE Communications Magazine*, vol. 61, no. 1, pp. 16–22, Jan. 2023.

[7] C. You and R. Zhang, "Wireless communication aided by intelligent reflecting surface: Active or passive?" *IEEE Wireless Commun. Lett.*, vol. 10, no. 12, pp. 2659–2663, Sep. 2021.

[8] R. Long, Y.-C. Liang, Y. Pei, and E. G. Larsson, "Active reconfigurable intelligent surface-aided wireless communications," *IEEE Trans. Wireless Commun.*, vol. 20, no. 8, pp. 4962–4975, Mar. 2021.

[9] Z. Zhang, L. Dai, X. Chen, C. Liu, F. Yang, R. Schober, and H. V. Poor, "Active RIS vs. passive RIS: Which will prevail in 6G?" *IEEE Trans. Commun.*, vol. 71, no. 3, pp. 1707–1725, Dec. 2023.

[10] G. Yang, X. Xu, Y.-C. Liang, and M. D. Renzo, "Reconfigurable intelligent surface-assisted non-orthogonal multiple access," *IEEE Trans. Wireless Commun.*, vol. 20, no. 5, pp. 3137–3151, Jan. 2021.

[11] T. Li, H. Zhang, S. Guo, and D. Yuan, "Max-min fair RIS-aided rate-splitting multiple access for multigroup multicast communications," *China Communications*, vol. 20, no. 1, pp. 184–198, Jan. 2023.

[12] Y. Mao, B. Clerckx, and V. O. Li, "Energy efficiency of rate-splitting multiple access, and performance benefits over SDMA and NOMA," in *2018 15th International Symposium on Wireless Communication Systems (ISWCS)*, Lisbon, Portugal 2018, pp. 1–5.

[13] H. Li, Y. Mao, O. Dizdar, and B. Clerckx, "Rate-splitting multiple access for 6GłPart III: Interplay with reconfigurable intelligent surfaces," *IEEE Communications Letters*, vol. 26, no. 10, pp. 2242–2246, Oct. 2022.

[14] R. Zhang, K. Xiong, Y. Lu, P. Fan, D. W. K. Ng, and K. B. Letaief, "Energy efficiency maximization in RIS-assisted SWIPT networks with RSMA: A ppo-based approach," *IEEE J. Sel. Areas Commun.*, vol. 41, no. 5, pp. 1413–1430, Jan. 2023.

[15] B. Makki, A. Graell i Amat, and T. Eriksson, "Green communication via power-optimized HARQ protocols," *IEEE Trans. Veh. Technol.*, vol. 63, no. 1, pp. 161–177, Jul. 2014.

[16] Z. Shi, S. Ma, G. Yang, and M.-S. Alouini, "Energy-efficient optimization for HARQ schemes over time-correlated fading channels," *IEEE Transactions on Vehicular Technology*, vol. 67, no. 6, pp. 4939–4953, Jun. 2018.

[17] S. W. H. Shah, A. N. Mian, S. Mumtaz, A. Al-Dulaimi, C.-L. I, and J. Crowcroft, "Statistical QoS analysis of reconfigurable intelligent surface-assisted D2D communication," *IEEE Trans. Veh. Technol.*, vol. 71, no. 7, pp. 7343–7358, Apr. 2022.

[18] S. Abidrabbu, S. R. Ali, and H. Arslan, "A novel HARQ design for RSMA networks," *IEEE Internet of Things Journal*, pp. 1–1, 2023.

[19] H. Niu, Z. Lin, K. An, J. Wang, G. Zheng, N. Al-Dhahir, and K.-K. Wong, "Active RIS assisted rate-splitting multiple access network: Spectral and energy efficiency tradeoff," *IEEE Journal on Selected Areas in Communications*, vol. 41, no. 5, pp. 1452–1467, May 2023.

[20] L. Yang, J. Yang, W. Xie, M. O. Hasna, T. Tsiftsis, and M. D. Renzo, "Secrecy performance analysis of RIS-aided wireless communication systems," *IEEE Trans. Veh. Technol.*, vol. 69, no. 10, pp. 12 296–12 300, Jul. 2020.

[21] M. K. Simon, *Probability Distributions Involving Gaussian Random Variables: A Handbook for Engineers, Scientists and Mathematicians*. Berlin, Heidelberg: Springer-Verlag, 2006.

[22] S. Primak, V. Kontorovich, and V. Lyandres, *Stochastic Methods and their Applications to Communications: Stochastic Differential Equations Approach*, West Sussex, U.K. : Wiley, 2004.